Epitaxially Textured $Pr_{0.6}Ca_{0.4}MnO_3$ Thin Films Under Considerably Low Substrate Temperature

M. Nyman[1], T. Elovaara[1], J. Tikkanen[1], S. Majumdar[12], H. Huhtinen[1]*, and Petriina Paturi[1]

[1] Wihuri Physical Laboratory, Department of Physics and Astronomy, University of Turku, FI-20014 Turku, Finland

[2] NanoSpin, Department of Applied Physics, Aalto University School of Science, P.O. Box 15100, FI-00076 Aalto, Finland

Abstract

We report the growth of well-crystallized and epitaxially textured $Pr_{0.6}Ca_{0.4}MnO_3$ thin films on $SrTiO_3$ substrates by pulsed laser deposition at considerably low substrate temperatures, as low as 450 °C, without high-temperature post-annealing treatments. Although a strong ferromagnetic interaction as well as a large irreversible metamagnetic transition with a training effect have been observed for films grown at 450 °C, the in-plane and out-of-plane lattice ordering is slightly improved with increasing substrate temperature. Therefore, a lowest magnetic field of 2 T for melting the insulating charge-ordering state at 70 K has been observed for films grown with the substrate temperature between 550 °C and 600 °C. The formation and growth of $Pr_{0.6}Ca_{0.4}MnO_3$ on $SrTiO_3$ substrate at exceptionally low substrate temperature is qualitatively modelled by the combination of the kinetic energies and redox potentials of the components of the ablation plasma, while the heat flow from the substrate is assumed to be less important.

Keywords: Small-bandwidth manganite, PCMO, Thin films, PLD, Substrate temperature, Growth mechanism

1 Introduction

The small-bandwidth manganite $Pr_{1-x}Ca_xMnO_3$ (PCMO), with fascinating electronical and magnetic properties like colossal magnetoresistance (CMR) [1, 2], coexistence of phase-separated regions [3], first order irreversible metamagnetic transition [4], large magnetocaloric effect [5, 6] and enormous resistive switching under optical or electrical excitation [7, 8, 9, 10, 11], has received a lot of technological and scientific interest. Especially, the stable and insulating charge-ordering (CO) state in the hole doping range of $x = 0.3 - 0.5$ [3, 12], which can be

---

*Corresponding author, email: hannu.huhtinen@utu.fi

Selection and peer-review under responsibility of the Scientific Programme Committee of ICM 2015

melted by an electric of magnetic field, can lead to an insulator-to-metal transition (IMT) where PCMO undergoes a metamagnetic first order phase transition from antiferromagnetic (AFM) to ferromagnetic (FM) phase. These phenomena have led to a huge potential in photovoltaic [13], magnetic data storage and memory applications [14]. However, the applications are based on high quality thin films and therefore the deposition process, where the substrate temperature plays a significant role, is one of the main focuses when developing multi-purpose films for future emerging energy technologies.

The structural and magnetic properties of the films are dictated by the prevailing environmental circumstances, the composition of the plasma plume and the properties of the substrate material during the ablation. The substrate-induced strain caused by a lattice mismatch has been observed to have dramatic effects on crystallographic symmetry as well as on the role of Mn–O–Mn bond angles in the formation of CO, orbital ordering (OO) and magnetic behaviour in PCMO films [15]. If the lattice mismatch is excessively large, epitaxial growth will not be able to take place, albeit an accurately controlled substrate temperature could provide sufficient surface mobility of the deposited material to ensure the thermodynamic and kinetic requirements for attaining the material with a correct stoichiometry under the background O_2 atmosphere. In principle, the substrate temperature defines the net heat flow out of the condensate. Thus a lowered substrate temperature will speed up the cooling and decrease the rate of crystallization of the material [16]. On the other hand, the substrate temperature should be low enough to prevent interlayer diffusion and film-substrate reactions, which weaken the properties of the films. Although the typical synthesizing temperatures have been around $1150 - 1350$ °C when traditional solid-state reaction to polycrystalline PCMO is used [17, 18, 19], Sarkar *et al.* have successfully synthesized $Pr_{0.5}Ca_{0.5}MnO_3$ nanoparticles at a much lower temperature ≈ 650 °C using a polymeric precursor route to obtain the perovskite phase [20]. According to the literature, the substrate temperature during PLD for well-crystallized and epitaxially textured PCMO films prepared without high-temperature annealing has varied between 700 and 800 °C [15, 19, 21, 22, 23].

In the present work, we explored the lower limits for the substrate temperature where epitaxially textured PCMO thin films could be manufactured. The variations in PCMO orientation, low-angle grain-boundaries and lattice ordering are investigated by x-ray diffractometry (XRD) and widely discussed with the results of magnetic properties.

2 Experimental details

A polycrystalline bulk target of $Pr_{0.6}Ca_{0.4}MnO_3$ was prepared with the ceramic method using high-purity powders of praseodymium (III,IV) oxide, calcium carbonate and manganese (III) oxide [24]. The PCMO films were grown on two different substrate materials, (100) $SrTiO_3$ (STO) and (100) MgO, having different lattice mismatch values with PCMO of 1.8 % and 9.9 % (tensile strain), respectively, by pulsed laser deposition (PLD) using an excimer XeCl 308 nm laser with a pulse duration of 25 ns. The laser fluence was 2 Jcm^{-2}, the repetition rate of the laser 5 Hz and the flowing oxygen pressure in the chamber 0.3 torr. The films were grown with a wide substrate temperature (T_s) range of $400 - 750$ °C for films on STO and $500 - 750$ °C for films on MgO, with *in situ* post-annealing treatment at each T_s for 10 min in atmospheric pressure of oxygen using heating and cooling rates of 25 °C/min. The thicknesses of the films were measured over chemically etched stripe edges by atomic force microscopy and within the resolution, the average thicknesses of all the films were ≈ 100 nm, thus independent on the substrate temperature.

The structural properties of the films were determined by XRD measured with a Philips

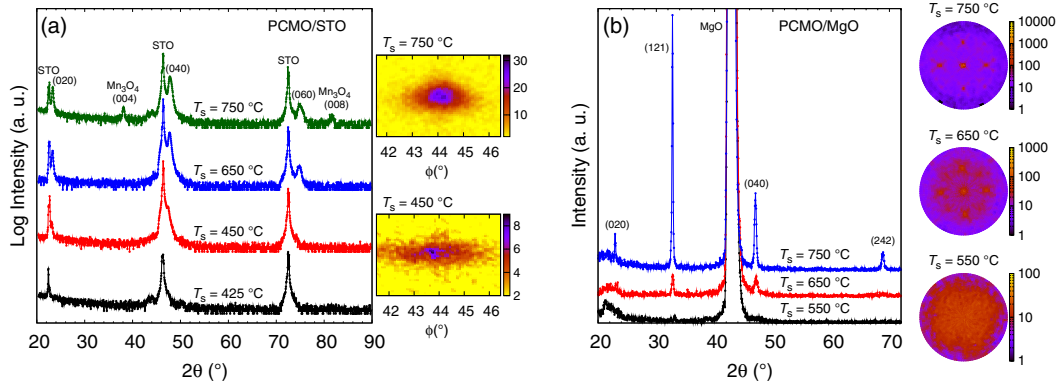Figure 1: The 2θ diffractograms of the PCMO films on STO (a) and MgO (b) at different T_s. (031) peaks as a function of 2θ and ϕ (with equivalent x and y ranges) are given for PCMO films on STO deposited at $T_\mathrm{s} = 450$ and $750\ ^\circ$C (a). The pole figures of the texture scans with relative intensities at $2\theta = 32.8^\circ$ for (121) peak of PCMO films on MgO with $T_\mathrm{s} = 550$, 650 and 750 $^\circ$C are given in (b).

X'Pert Pro MPD system. To determine the phase purity of the films and the orientation of the PCMO, $\theta - 2\theta$ scans in $(0k0)$ direction were made. The lattice parameters were determined from detailed 2D $(\phi, 2\theta)$ texture scans of PCMO (112)/(031) peaks for films on STO and (121) and (040) peaks for films on MgO, using 2D Levenberg-Marquardt fitting [25] of Gaussian peaks. The out-of-plane crystallographic texture was determined by XRD rocking curves (RC) of PCMO (060) peaks (ω scans). The magnetic measurements were made with a Quantum Design MPMS SQUID magnetometer measuring the temperature dependences of zero-field-cooled (ZFC) and field-cooled (FC) magnetizations in the field of 100 mT. The virgin magnetizations as functions of the external magnetic field B and magnetic hysteresis curves were recorded at -5 T $\leq B \leq$ 5 T at temperatures of 10, 30, 50, 70, 100 and 250 K. The external field B was always oriented along the planes of the films, along the PCMO [101] axis.

3   Results and discussion

3.1   Structural properties

From the 2θ diffractograms shown in Fig. 1 we can observe that for films on STO at $T_\mathrm{s} = 425\ ^\circ$C no PCMO peaks can be detected, but at $450\ ^\circ$C $\leq T_\mathrm{s} \leq 750\ ^\circ$C the PCMO $(0k0)$ reflections are seen. This is in line with earlier results where PCMO on STO substrate energetically optimizes itself by having the longest lattice vector **b** out-of-plane and vectors **a** and **c** in-plane along the diagonal of the unit cell base [19]. However, the T_s dependent shift and the evidently resulting separation of PCMO peaks from STO $(00l)$ peaks can be observed. This indicates that, at higher T_s, the PCMO lattice relaxes itself better towards its own bulk values and the influence of the STO substrate diminishes. When looking at the diffractogram for the film deposited at 750 $^\circ$C, clearly noticeable peaks at $2\theta = 38.7^\circ$ and 81.5° can be observed. These maxima indicate the Mn_3O_4 impurity phase [26] and its formation at high T_s seems to be related to the growth process, since in the target material the impurities cannot be detected. Albeit it is extremely difficult to determine the absolute amount of Mn_3O_4 impurity, its tetragonal unit
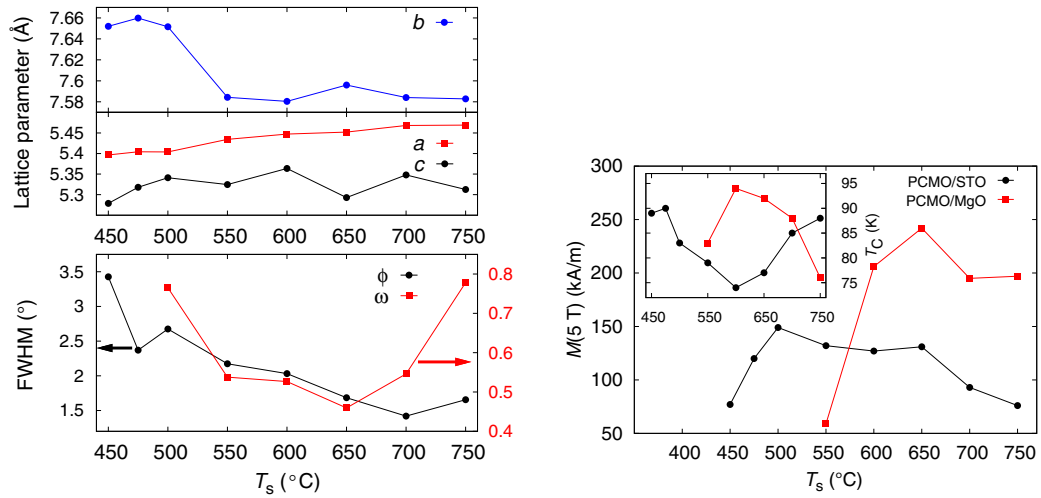
Figure 2: (a) T_s dependence of the room temperature lattice parameters a, b and c, and the peak full widths at half-maximum (FWHM) in ϕ direction as well as the width of the PCMO (060) rocking curve $\Delta\omega$ at different T_s. (b) T_s dependence of the saturation magnetization determined in the field of 5 T (M_{5T}) from the hysteresis loops at 70 K for PCMO films deposited on STO and MgO substrates (main panel). The inset shows the Curie temperature T_C vs. T_s calculated from the first derivatives of M_{FC} curves.

cell with the longest lattice vector **c** out-of-plane can be obtained from the analysis.

The positions of the PCMO peaks in 2θ diffractograms as well as their full widths at half maximum (FWHM) were determined by fitting a pseudo-Voigt function to the peaks [27]. As can be seen from the upper panel of Fig. 2(a), the longest b parameter is around 7.65 Å at 450 °C $\leq T_s \leq 500$ °C and it shortens remarkably to the value of 7.58 Å for $T_s = 550$ °C, being almost constant above this when T_s is increased up to 750 °C. Contrary to this, the lattice parameter a increases slightly but almost linearly with increasing T_s, from the value of 5.40 Å at $T_s = 450$ °C to 5.47 Å at $T_s = 750$ °C. For c, a shortening can be observed at $T_s < 500$ °C, while c remains more or less constant within the error bars when $T_s > 500$ °C. However, the volume of the unit cell seems to stay approximately constant, regardless of the used T_s. In general, the lattice parameters for these relatively thin films are comparable with the values observed earlier for PCMO powders [28] as well as for the values of the bulk target used in our PLD process [4], which are $a = 5.43$ Å, $c = 5.41$ Å and $b = 7.64$ Å, respectively. The tensile strain induced by the STO substrate should increase the average of the PCMO in-plane parameters a and c, but this is realized only in the parameter a at substrate temperatures $T_s > 550$ °C. The decrease of the lattice parameters is usually explained by the increased amount of Mn^{4+} ions in the films, formed during the *in situ* annealing treatment in oxygen where the amount of cation-oxygen-cation bonds is increased. At the same time, the average length of the bonds decreases and the oxygen content is increased in the lattice [29, 30].

From the XRD 2D-measurements, the crystalline quality, including the presence of possible defects such as twin-boundaries or low-angle grain boundaries can be evaluated. As can be seen from the lower panel of Fig. 2(a), the width of the (031) peak in the ϕ-direction decreases almost linearly with increasing T_s, having the smallest $\Delta\phi \approx 1.5°$ at $T_s \geq 700$ °C. A clear difference

between the samples with $T_s = 450$ °C and 750 °C and thus a tendency for peak widening can be seen in the $2\theta - \phi$ scans of the (031) peaks shown on the right side of Fig. 1 (a). This is a clear indication that the higher T_s decreases the amount of low-angle grain boundaries while at low T_s the adatoms do not have enough thermal energy to orient the crystals fully parallel to each other [29]. The out-of-plane ordering is determined from the rocking-curve measurements of (060) peaks where the clearly narrowest peaks with $\Delta\omega \approx 0.5°$ can be observed at 550 °C $\leq T_s \leq 700$ °C (the lower panel of Fig. 2), while the $\Delta\omega$ value increases remarkably below and above this T_s. Below $T_s = 500$ °C, the $\Delta\omega$ values are not reliable anymore, since the signal is relatively weak and noisy. The results indicate that the out-of-plane crystalline texture and the long-range lattice ordering explicitly weaken outside the optimal T_s.

As a comparison, the structural properties are also characterized for PCMO films deposited on MgO with higher lattice mismatch, and an informative summary of the effect of T_s is shown in Fig. 1 (b). Below $T_s < 550$ °C, the PCMO diffraction maxima cannot be observed but already at $T_s = 550$ °C a small hump at $2\theta = 32.8°$, indicating the PCMO (121) reflection, can be seen. The intensity of the peaks corresponding to this family of lattice planes obviously strengthens with increasing T_s. Above $T_s \geq 650$ °C also the peaks from the family of $\{0k0\}$ reflections start to appear at $2\theta = 22.9°$ and $47.1°$, indicating at least these two preferred orientations for the films on MgO. As an example, the pole figures obtained from the texture scans of the PCMO (121) reflections with relative intensities are given on the right side of Fig. 1 (b) at substrate temperature $T_s = 550$ °C, 650 °C and 750 °C. From these figures, we can conclude that the crystalline ordering obviously improves with increasing T_s. This can be detected based on the decreased amount of indefinite background and the appearance of clearly focused and sharpened peak maxima with high intensities at high T_s [31]. In practise at $T_s = 750$ °C, the growth process is not random since three different preferred crystalline orientations can be indentified where [010], [220] and [121]-directions are situated out-of-plane from the face of the film surface. In addition, a part of the [010]-oriented crystals are rotated by $45°$ in-plane, some [220]-oriented crystals are rotated by $\pm45°$ and some [121]-oriented crystals by $\pm10°$, $\pm45°$ or $\pm100°$, respectively. When taking into account the peak intensities together with the static structure factors of PCMO, we can conclude from the pole figures that the most probable orientation by far is to have the lattice vector **b** out-of-plane.

3.2   Magnetic properties

An excellent illustration of the influence of T_s on the magnetic properties over the PCMO growth mechanism on the STO substrate can be seen in Fig. 3(a) where indications of an at least partially FM ground state together with a thermomagnetic irreversibility (TMI) can be observed for films with $T_s \geq 450$ °C. This is in line with earlier measurements for PCMO thin films [23], where FM at low temperature could result from spin canting, a spin-glass phase or the existence of FM clusters within the AFM matrix [3, 15]. The FC magnetization observed in 100 mT field at 10 K increases with T_s, having the highest value at $T_s = 500$ °C and decreasing slightly between $T_s = 550$ and 650 °C until the ferrimagnetic Mn_3O_4 impurity phase starts to occur at $T_s \geq 650$ °C, increasing the total FM response. A similar effect can seen from the irreversibility of magnetization, $M_{irr} = M_{FC} - M_{ZFC}$, where the highest M_{irr} can be observed at $T_s = 500$ °C (not shown).

In all PCMO films with $T_s \geq 450$ °C, a clear maximum in the ZFC curve appears around 50 K, above which the magnetization drops following the FM–paramagnetic (PM) transition. The earlier observed CO and OO transitions around 250 K with $x = 0.3-0.5$ cannot be observed here, as also reported previously [21]. This can be explained by the cooperative Jahn-Teller
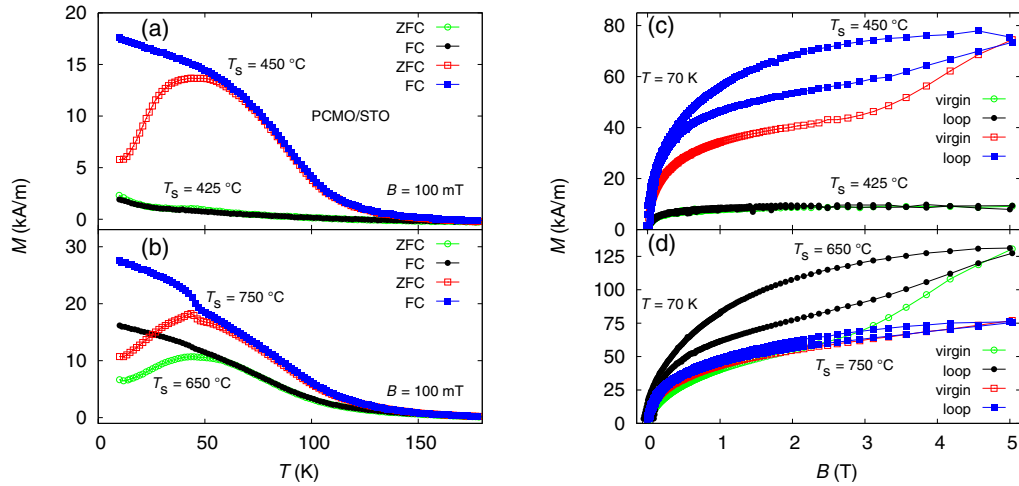
Figure 3: Temperature dependence of the M_{ZFC} and M_{FC} magnetizations ($B = 100$ mT) for PCMO on STO substrate at $T_s = 425$ °C, 450 °C (a) and 650 °C, 750 °C (b). (c) and (d) illustrate the positive field branches of the loops with virgin curves at 70 K, respectively.

Figure 4: Temperature dependence of the M_{ZFC} and M_{FC} magnetizations ($B = 100$ mT) for PCMO on MgO substrate at $T_s = 500$ °C, 550 °C (a) and 650 °C, 750 °C (b). (c) and (d) illustrate the positive field branches of the loops with virgin curves at 70 K, respectively.
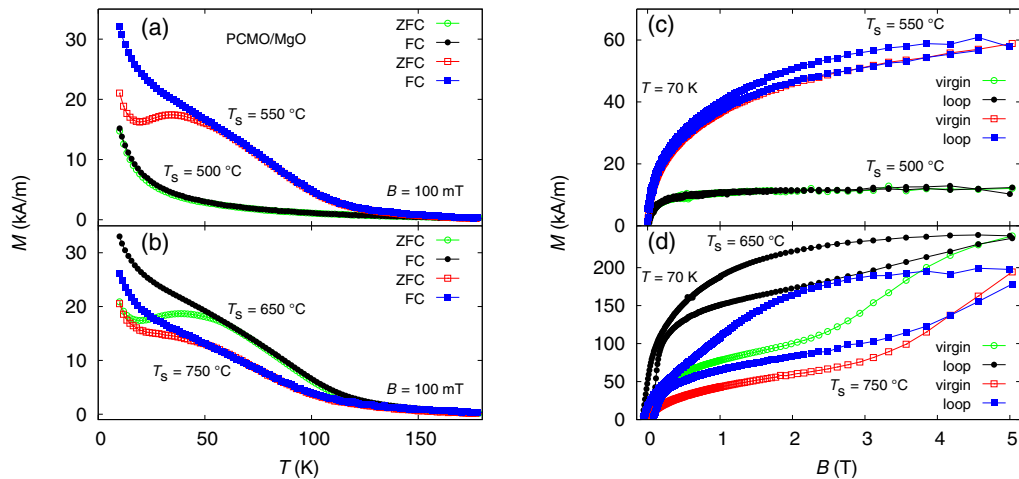
(JT) distortion of the MnO_6 octahedra which is modified by the substrate lattice induced strain in thin films [4, 32]. At $T_s \geq 650$ °C in both ZFC and FC curves, one can see a precipitous upturn around 45 K, which becomes more pronounced with increasing T_s. This phenomenon can be connected to the formation of a Mn_3O_4 impurity which shows ferrimagnetic behaviour with a slightly shifted T_N around 43 K [33, 34].

As can be seen from the virgin curves and the hysteresis loops measured at 70 K (Fig. 3(b)), an obvious magnetic irreversibility, indicating a metamagnetic transition, occurs at $T_s \geq 450$ °C. Also at 450 °C $\leq T_s \leq 700$ °C, the measurements confirm the presence of a so-called training effect where obviously different routes between the virgin and subsequent field curves can be observed. In addition, the clear difference between the slopes on both sides of the 3 T field in the virgin curves is connected to the competition between FM and AFM phases where long-range FM ordering slowly starts to dominate, simultaneously melting the CO state. When the external field is decreased again, the reverse route follows the typical FM behaviour, which shows the signs of a first order phase transition and a metastable FM phase in PCMO thin films. These phenomena are widely discussed in our previous paper [21]. The observed onset melting field of the CO state at 70 K, B_M, is around 3.3 T for films with $T_s = 450$ °C and 475 °C. Above this T_s range, B_M starts to decrease reaching its smallest value of ≈ 2 T at 550 °C $\leq T_s \leq 600$ °C, above which B_M increases again back to the value of 3 T at $T_s = 650$ °C. This is in line with the structural properties where a reduced amount of crystalline defects is observed with increased T_s and an impurity phase is observed at $T_s \geq 650$ °C. However, the steepest CO state melting transition is observed for the sample with $T_s = 500$ °C, which also has the highest magnetization at low temperatures as observed earlier in the temperature dependence measurements.

The general effects of T_s on the magnetic characteristics of PCMO films grown on MgO substrate are presented in Fig. 4. At the low $T_s = 500$ °C, mainly a PM background signal from the MgO can be seen in the $M(T)$-curves. Above this T_s, FM behaviour exists up to the highest $T_s = 750$ °C although the signal level starts to diminish above $T_s = 700$ °C. However, when comparing the M values with the films grown on STO substrates, we can conclude that the higher magnetizations in PCMO films on MgO can be related to the larger amount of grain-boundaries which could re-orient the magnetic domains in the grains or produce disorder-induced canting of Mn spins in the grain-boundary region [35]. In contrast with the films on STO, no anomalies that could be related to Mn_3O_4 impurities can be observed in the films on MgO. From the hysteresis loops, we can see that the magnetic irreversibility increases with increasing T_s, showing clearly opened hysteresis loops especially at $T_s = 750$ °C. On the other hand, the training effect reaches its maximum at $T_s = 750$ °C where an obviously different virgin curve trace can be seen. In addition, the B_M of the CO state increases with increasing T_s, being 2.3 T for $T_s = 650$ °C, 2.8 T for $T_s = 700$ °C and over 3 T for PCMO grown on MgO at $T_s = 750$ °C. These observations are in agreement with each other where the films wih a small melting field also have a more persistent FM state at this temperature, which again is manifested by the smaller magnetic irreversibility in the high field loops.

The effect of T_s on two critical parameters, the Curie temperature, T_C, and the saturation magnetization, M_{5T}, are shown in Fig. 2(b). As can be seen from the inset, the T_C of PCMO on STO decreases from around 90 K for $T_s = 450$ °C down to the minimum value of 75 K at $T_s = 600$ °C and increases again back to ≈ 90 K for the film with $T_s = 750$ °C. A reverse phenomenon can be observed for films on MgO, where T_C achieves the maximum value of ≈ 94 K at $T_s = 600$ °C, having clearly lower values at the both ends of the used T_s range. For PCMO on STO, the decrease in T_C with increasing T_s can be understood by the reduced amount of crystalline defects which, due to the thermal motion, allows the spins to orient without restrictions [36]. However, the increase in T_C at $T_s > 600$ °C can be explained by the appearance of Mn_3O_4 impurities at $T_s \geq 600$ °C which allows the spins to become trapped close to them, requiring a higher temperature for re-orientation [37]. The saturation magnetization values in 5 T field are presented in the main panel of Fig. 2(b). For PCMO on STO, M_{5T} increases within the substrate temperature range 450 °C $\leq T_s \leq 500$ °C, being approximately constant until the

Mn_3O_4 impurity phase starts to take effect by reducing the M_{5T} value again at $T_s \geq 650$ °C. For PCMO on MgO, the improved crystallization above $T_s = 550$ °C is reflected by the increased M_{5T} values, which remain unchanged up to the highest used T_s of 750 °C.

3.3   Discussion

The PCMO films on STO were crystallographically of good quality, well-textured and epitaxially grown on small lattice mismatch inducing STO with the growth temperature range of $450 - 600$ °C, while above this temperature the Mn_3O_4 impurity phase starts to appear among the PCMO matrix. The substrate temperature of 450 °C, significantly lower than observed earlier for complex oxide thin films grown by PLD $(700 - 800$ °C$)$, is of extreme importance for practical applications with cost-effective and technologically greener production of electronic components. However, our present understanding of the nucleation and growth processes at the low substrate temperatures observed in this work is far from being a self-explanatory model.

The constituent particles of the PLD plasma plume have high kinetic energies and a positive average electric charge before they reach the substrate. It is therefore improbable that significant PCMO crystal growth could occur in the plasma phase. The critical chemical reactions that lead to the formation of the PCMO phase, and its epitaxial crystallization, must mainly occur at the surface of the substrate. In a simple model, one can think of three possible sources for the activation energies required by these reactions: the thermal energy of the substrate, the kinetic energy of the precursor particles, and the redox potentials of the precursors. Our present findings indicate that, of these, the heat flow from the substrate is not critical for the formation of the PCMO phase. This can be inferred from the fact that at 450 °C, the substrate is way below the minimum temperature of 650 °C that is reportedly required for the thermal activation of solid-state PCMO synthesis [20]. We presume that the most important function accomplished by heating the substrate is simply to allow new adatoms to migrate effectively towards a minimum energy configuration, improving the epitaxiality of the growing film.

What activates the formation of PCMO, then, must be a combination of the kinetic energies and redox potentials of the components of the PLD plasma. The minuscule mass flow of the plasma is too small to cause a significant heating of the substrate surface as a whole, but nevertheless, the kinetic energy of the precursor particles may play a role in the dynamics of the synthesis reaction, as the kinetic energy is dissipated into heat and, possibly, further ionizations during individual particle collisions. However, such processes are difficult to quantify without knowing the exact composition and energy spectrum of the plasma. On the other hand, it turns out that the redox potentials of the metal ions contained in the plasma could suffice for explaining the formation of PCMO already at 450 °C. A related manganite compound, $La_{0.5}Ba_{0.5}MnO_3$, has been successfully synthesized at 240 °C using a hydrothermal method [38], *i.e.* by heating an alkaline water solution of metal salts. The analogy of this method to our PLD, if admittedly a coarse one, lies in the fact that the PLD plasma plume, akin to a water solution, already contains a significant portion of the metals in their reactive, ionized states. In principle, this allows most of the energy required for the PCMO synthesis to be stored in the redox potentials of the precursor ions at the time they are explosively ablated from the PLD target.

Aside from the successful synthesis of PCMO thin films at unconventionally low substrate temperatures, the other significant finding of our present study was the systematic development of an impurity phase recognized as hausmannite, Mn_3O_4, among PCMO grown on STO, when the substrate temperature was increased above 600 °C. This is an unexpected result, in that Mn_3O_4 should be unstable against further oxidation into bixbyite, α-Mn_2O_3, in the temperature

range $600 - 900$ °C [39]. The discrepancy must be resolved by assuming that the oxygen annealing process, lasting only 10 min for each film, is too brief to allow the impurity phase to reach its thermodynamic equilibrium. The reason for Mn_3O_4, or manganese(II,III) oxide, to appear in the first place could be that despite the presence of a small amount of molecular oxygen, the near-vacuum film growth conditions facilitate the reduction of some Mn^{3+} and Mn^{4+} ions down to the oxidation state Mn^{2+} before any PCMO can form. This kind of a reduction process, not surprising for metal oxides [40], would naturally be faster and more prominent at higher temperatures. The occurence of this reduction only on STO substrate is a probable indication that the reduction is catalyzed by the STO substrate material. It is known that perovskite manganites can remain stable despite a small Mn deficiency [41], explaining the absence of any further phases besides Mn_3O_4 and PCMO.

4   Conclusions

The growth mechanism of pulsed laser deposited small-bandwidth $Pr_{0.6}Ca_{0.4}MnO_3$ (PCMO) manganite thin films is studied on two different substrate materials, $SrTiO_3$ and MgO, both of which induce tensile strain. The most critical growth parameter, the substrate temperature, is optimized over a wide temperature range. In PCMO films on STO, well-crystallized and epitaxially textured films have been deposited at temperatures as low as 450 °C without any high-temperature post-annealing treatment, although the improvement of in-plane and out-of-plane lattice ordering has been observed with increasing substrate temperatures. Additionally for thin films deposited at low temperatures, a strong ferromagnetic interaction as well as a large irrereversible metamagnetic transition with a training effect have been observed where the insulating charge-ordering state can be melted by applying a relatively low magnetic field of around 2 T at 70 K. On the other hand, for PCMO films on MgO, epitaxial growth cannot be realized and different crystal orientations can therefore be detected in the whole substrate temperature range used.

The nucleation and epitaxial crystallization of the PCMO films on STO at such exceptionally low substrate temperatures is explained by the combination of the kinetic energies and redox potentials of the components of the plasma plume, while the heat flow from the substrate is assumed to be less important. In addition, the formation of Mn_3O_4 impurity phase, at a relatively high substrate temperature but only on STO substrates, is connected with the reduction of Mn^{3+} and Mn^{4+} ions down to the oxidation state Mn^{2+} catalyzed by the STO substrate material at a relatively low molecular oxygen pressure.

Acknowledgements

References

[1] S. Jin, R. C. Sherwood, E. M. Gyorgy, T. H. Tiefel, R. B. van Dover, S. Nakahara, Appl. Phys. Lett. 54 (1988) 584.

[2] A.-M. Haghiri-Gosnet, J.-P. Renard, J. Phys. D.:Appl. Phys. 36 (2003) R127.

[3] A. Dagotto, T. Hotta, A. Moreo, Physics Reports 344 (2001) 1.

[4] T. Elovaara, H. Huhtinen, S. Majumdar, P. Paturi, J. Phys. Cond. Mat. 24 (2012) 216002.

[5]   M. S. Reis, V. S. Amaral, J. P. Araujo, P. B. Tavares, A. M. Gomes, I. S. Oliveira, Phys. Rev. B 71 (2005) 144413.

[6]   V. S. Kolat, T. Izgi, A. O. Kaya, N. Bayri, H. Gencer, S. Atalay, J. Magn. and Magn. Mater. 322 (2010) 427.

[7]   K. Miyano, T. Tanaka, Y. Tomioka, Y. Tokura, Phys. Rev. Lett. 78 (1997) 4257.

[8]   M. Fiebig, K. Miyano, T. Satoh, Y. Tomioka, Y. Tokura, Phys. Rev. B 60 (1999) 7944.

[9]   S.-L. Li, Z. L. Liao, J. Li, J. L. Gang, D. N. Zheng, J. Phys. D: Appl. Phys. 42 (2009) 045411.

[10] S. Majumdar, H. Huhtinen, M. Svedberg, P. Paturi, S. Granroth, K. Kooser, J. Phys. Cond. Mat. 23 (2011) 466002.

[11] S. Majumdar, T. Elovaara, H. Huhtinen, S. Granroth, P. Paturi, J. Appl. Phys. 113 (2013) 063906.

[12] Y. Tokura, Colossal magnetoresistive oxides, Gordon and Breach Science, New York, 2000.

[13] P. Beaud, A. Caviezel, S. O. Mariager, L. Rettig, G. Ingold, C. Dornes, S.-W. Huang, J. A. Johnson, M. Radovic, T. Huber, T. Kubacka, A. Ferrer, H. T. Lemke, M. Chollet, D. Zhu, J. M. Glownia, M. Sikorski, A. Robert, H. Wadati, M. Nakamura, M. Kawasaki, Y. Tokura, S. L. Johnson, U. Staub, Nature Materials 13 (2014) 923.

[14] Y. Murakami, H. Kasai, J. J. Kim, S. Mamishin, D. Shindo, S. Mori, A. Tonomura, Nature Nanotechnology 5 (2010) 37.

[15] C. S. Nelson, J. P. Hill, D. Gibbs, M. Rajeswari, A. Biswas, S. Shinde, R. L. Greene, T. Venkatesan, A. J. Millis, F. Yokaichiya, C. Giles, D. Casa, C. T. Venkataraman, T. Gog, J. Phys. Cond. Mat. 16 (2004) 13.

[16] B. Roas, L. Schultz, G. Endres, Appl. Phys. Lett. 53 (1988) 1557.

[17] Z. Jirak, J. Hejtmanek, K. Knizek, M. Marysko, E. Pollert, M. Dlouha, S. Vratislav, R. Kuzel, M. Hervieu, J. Magn. and Magn. Mater. 250 (2002) 275.

[18] M. R. Lees, J. Barratt, G. Balakrishnan, D. M. Paul, C. D. Dewhurst, J. Phys. Cond. Mat. 8 (1996) 2967.

[19] M. Svedberg, S. Majumdar, H. Huhtinen, P. Paturi, S. Granroth, J. Phys. Cond. Mat. 23 (2011) 386005.

[20] T. Sarkar, P. K. Mukhopadhyay, A. K. Raychaudhuri, J. Appl. Phys. 101 (2007) 124307.

[21] T. Elovaara, T. Ahlqvist, S. Majumdar, H. Huhtinen, P. Paturi, J. Magn. and Magn. Mater. 381 (2015) 194.

[22] W. Prellier, A. M. Haghiri-Gosnet, B. Mercey, P. Lecoeur, M. Hervieu, C. Simon, B. Raveau, Appl. Phys. Lett. 77 (2000) 1023.

[23] T. Mertelj, R. Yusupov, M. Filippi, W. Prellier, D. Mihailovic, Appl. Phys. Lett. 93 (2008) 042512–1.

[24] J. Tikkanen, H. Huhtinen, P. Paturi, J. Alloys Comp. 635 (2015) 41.

[25] W. H. Press, B. P. Flannery, S. A. Teukolsky, W. T. Vetterling, Numerical Recipes in C: The Art of Scientific Computing, Cambridge University Press, 1990.

[26] V. Markovich, I. Fita, R. P. C. Martin, A. Wisniewski, C. Yaicle, A. Maignan, G. Gorodetsky, Phys. Rev. B 73 (2006) 224423.

[27] J. Rodriguez-Carvajal, FULLPROF: a program for Rietveld refinement and pattern matching analysis, Abstracts of the Satellite Meeting on Powder Diffraction of the XV Congress of the IUCr (1990) 127.

[28] M. R. Lees, J. Barrat, G. Balakrishnan, D. M. Paul, C. Ritter, Phys. Rev. B 58 (1998) 8694.

[29] S. Majumdar, H. Huhtinen, S. Granroth, P. Paturi, J. Phys. Cond. Mat. 24 (2012) 206002.

[30] J. B. Goodenough, Physical Review 100 (1955) 564.

[31] U. F. Kocks, C. N. Tome, H.-R. Wenk, Texture and anisotropy : preferred orientations in polycrystals and their effect on materials properties, Cambridge University Press, 2000.

[32] F. Duan, J. Guojun, Introduction to Condensed Matter Physics, Volume 1, World Scientific Pub-

lishing, 2005.

[33] P. Z. Si, D. Li, C. J. Choi, Y. B. Li, D. Y. Geng, Z. D. Zhang, Solid State Communications 142 (2007) 723.

[34] H. Zhang, C. Liang, Z. Tian, G. Wang, W. Cai, Journal of Physical Chemistry C 114 (2010) 12524.

[35] A. Gupta, G. Q. Gong, G. Xiao, P. R. Duncombe, P. Lecoeur, P. Trouilloud, Y. Y. Wang, V. P. Dravid, J. Z. Sun, Phys. Rev. B 54 (1996) R15629.

[36] J. M. D. Coey, Magnetism and magnetic materials, Cambridge University Press, 2010.

[37] F. Brailsford, Physical Principles of Magnetism, D. Van Nostrand Company LTD., 1966.

[38] Sulje ikkuna J. Spooren, A. Rumplecker, F. Millange, R. I. Walton, Chemistry of Materials 15 (2003) 1401.

[39] F. A. al Sagheer, M. A. Hasan, L. Pasupulety, M. I. Zaki, Journal of Materials Science Letters 18 (1999) 209.

[40] S. Y. Lee, N. Mettlach, N. Nguyen, Y. M. Sun, J. M. Applied Surface Science 206 (2003) 102.

[41] S. Hebert, B. Wang, A. Maignan, C. Martin, R. Retoux, B. Raveau, Solid State Communications 123 (2002) 311.